Available online at www.sciencedirect.com
SCIENCE DIRECT®
International Journal of Machine Tools & Manufacture 44 (2004) 1619–1628
INTERNATIONAL JOURNAL OF MACHINE TOOLS & MANUFACTURE DESIGN, RESEARCH AND APPLICATION
www.elsevier.com/locate/ijmactool

Process synthesis of laser forming by genetic algorithm

J. Gary Cheng [a,*], Y. Lawrence Yao [b]

[a] School of Mechanical and Materials Engineering, Washington State University, Pullman, WA 99164, USA
[b] Department of Mechanical Engineering, Columbia University, New York, NY 10027, USA

Received 8 December 2003; accepted 2 June 2004

Abstract

Significant progress has been made in analyzing and predicting laser forming (LF) processes of sheet metal. Process synthesis in laser forming, on the other hand, is concerned with determination of laser scanning paths and heat condition given a target shape to form. This paper reports the development of a process synthesis methodology for laser forming of a class of shapes based on genetic algorithm (GA). The effects of GA control parameters on the synthesis process are discussed. The effects of fitness function types on achieving multiple objectives are also investigated. The synthesis process is experimentally validated through several cases under diverse conditions including one that involves close to thirty decision variables.

Keywords: Process synthesis; Laser forming; Genetic algorithm; Optimization; Multiobjective; FEM

1. Introduction

A laser forming (LF) process is characterized by various process parameters such as laser scanning paths and heating conditions including laser power and scanning velocity. Making proper decisions regarding controllable process parameters is the main problem that a process designer is faced with. Much research has been done to analyze deformation and residual stress given laser scanning paths and heating conditions. For instance, numerical and experimental investigations have been carried out to better understand laser forming process mechanisms and the effects of key process parameters on dimension and mechanical properties of the formed parts [1–4]. Temperature and strain-rate dependent material properties have been considered in the numerical models for laser forming processes [5]. Convex laser bending based on buckling mechanism has been investigated [6]. Microstructure dependent flow stress has been integrated in FEM simulation of laser forming process [7].

For laser forming to become a practical process, however, the issue of process synthesis needs to be addressed, that is, designing laser scanning paths and heating conditions for a given shape. Unlike traditional machining, where cutter paths are readily determined by offsetting a distance from the given part geometry, process planning for laser forming is less obvious especially for general 3D shapes. This is primarily because laser forming induced deformation has its own characteristics, and how to link them to the strain field required to form the given part is generally not obvious. In addition, like many inverse problems, process planning for LF has multiple solutions. A method developed by Shimizu [8] used genetic algorithms (GAs) to decide the laser heating paths, laser power, and scanning velocity to form a simple domed shape. However, the decision variables are set as discrete values and the assumptions made were rather restrictive leading to inflexible solutions. It also experienced difficulty when experimental validation of the result was attempted. Hennige [9] and Magee et al. [10] experimentally investigated the scanning patterns for spherical shapes. Based on prior knowledge of the laser forming process, radial and concentric scanning paths were postulated and tested. Advantages and disadvantages of each as well as their various combinations were shown and compared. Other process parameters were only dealt with marginally.

GAs, which are optimization techniques based on probabilistic transition rules, have been successfully

* Corresponding author. Tel./fax: +1-509-335-4662.
E-mail address: cheng1@wsu.edu (J.G. Cheng).

0890-6955/$ - see front matter © 2004 Elsevier Ltd. All rights reserved.
doi:10.1016/j.ijmachtools.2004.06.002

implemented for a wide range of problems in physical and social sciences, engineering and operations research, and computer sciences [11,12]. GAs mimic the natural evolution process by which superior creatures evolve while inferior ones fade out from the population as generations go on. GAs have been proved to be a robust, simple-to-implement method, which can handle a large set of parameters. The disadvantages of GAs include their long computational time, and the semi-empirical nature of the algorithm parameter selection procedure. There have been reports on GAs' applications in process design for metal working. Chung and Hwang [13] presented a GA based approach for process optimal design in hot forging, in which non-isothermal process parameters were optimally determined. Roy et al. [14] applied GAs to optimal design of process variables in multi-pass wire drawing. They proposed micro-genetic algorithms (μGAs) and applied the adaptive algorithms to the design process. By choosing different objective functions, the GA based optimization resulted in reduction of the number of passes, reduction in total deformation energy, and improved uniformity in effective plastic strain and temperature distribution.

In this paper, a GA based approach is presented for process synthesis applicable to laser forming of a class of shapes. The synthesis scheme developed in this study has the advantage of being able to handling a large number of decision variables. This approach is validated through several cases. The effects of fitness function and control parameters of GAs (population size, crossover rate and mutation rate) on the convergence of the design process are also investigated.

2. Necessity of a heuristic approach

Given laser power P, scanning speed V, and beam diameter D, as well as geometric attributes of sheet metal ξ, laser scanning paths ψ, and material properties ζ, the temperature distribution in the sheet metal being irradiated by a scanning laser beam may be explicitly expressed as

$$T = f(x,y,z,t,P,V,D,\xi,\psi,\zeta) \tag{1}$$

where x, y, z are the coordinates in X, Y, Z directions, respectively, shown in Fig. 1(a), and t is he thickness of the sheet. An example is the well-known steady-state solution to the moving heating source problem, where a line heating source scans the surface of a metal sheet with constant speed. The temperature distribution can be expressed as:

$$T = \frac{Q}{2\pi\lambda t}\exp\left(\frac{Vw}{2a}\right)K_0\left(\frac{Vr}{2a}\right) \tag{2}$$

where Q, λ, t, and a are heat input per unit time, thermal conductivity, sheet metal thickness, and thermal

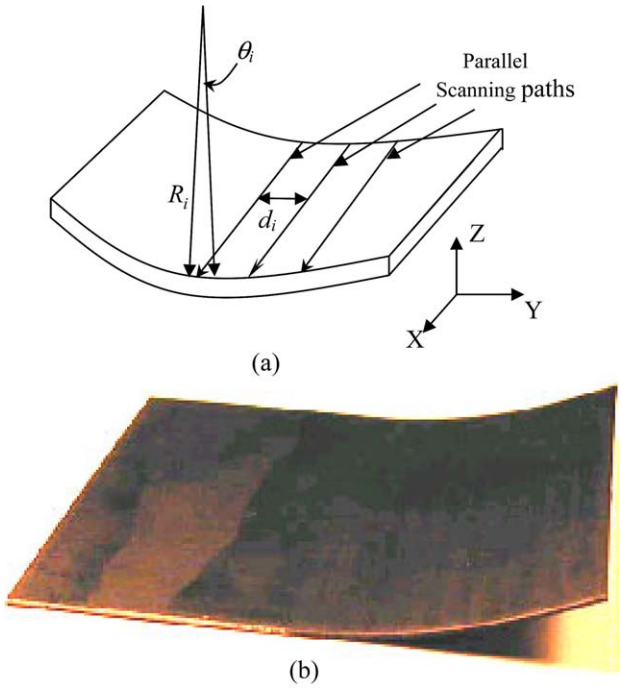

Fig. 1. (a) Schematic of a class of shapes and parallel scanning paths; and (b) sheet metal after laser formed using the scanning paths in (a) (half of the sheet is formed assuming symmetry).

diffusivity, respectively; K_0 is second kind Bessel function of zero order; V is the velocity of the moving heating source; r is the radial distance from the heat source center; and w is the distance from heating source center along scanning direction. There are no close-form solutions like Eq. (2) for more complex situations but numerical solutions can be sought.

The explicit expression of deformation as a result of the temperature distribution

$$U_{x,y,z} = g(T,x,y,z,t,\xi,\zeta) \tag{3}$$

is, however, generally unobtainable. For one thing, this is because T could contain a form of Bessel function (Eq. (2)). As a result, $U_{x,y,z}$ cannot be explicitly expressed as a function of scanning paths and heating conditions and requires methods like finite element modeling or finite difference modeling to solve [3,7].

As a result, analytically or even numerically solving the inverse problem, that is, determining the scanning path and heat condition in terms of P, V, D, and ψ given desired deformation $U_{x,y,z}$ is obviously even less feasible. This is why heuristic approaches such as GAs provide a viable alternative. GAs differ from traditional search and optimization methods in the following aspects. GAs use probabilistic transition rules, not deterministic ones and therefore do not require derivative information or other auxiliary knowledge; only the objective function and corresponding fitness levels influence the directions of search; GAs search a

population of points in parallel, therefore, GAs are traveling in a search space with more individuals, and are less likely to get stuck in a local extreme like some other methods; and GAs can handle large sets of parameters including discrete ones.

3. Problem description

In this study, a class of target shapes is chosen to investigate the feasibility of using GAs for process synthesis of laser forming. As shown in Fig. 1a, the class of target shapes assumes a general 2D profile in the Y–Z plane while the profile remains unchanged in the X direction. The class is chosen to allow relative simplicity without loss of generality. It is further assumed that the target shapes can be formed by a laser-scanning pattern ψ consisting of straight-lines parallel to each other and to the X-axis.

The decision variables, therefore, are N is the number of parallel scan lines; P_i ($i = 1$–N) is the laser power at the ith scan; V_i ($i = 1$–N) is the laser-scanning velocity at the ith scan; d_i ($i = 1$–N) is the distance between the ith and $(i+1)$th scan lines or the sheet edge. Laser beam size D is assumed constant. This implies that the given shape will be either concave or convex. The value of D in relation with sheet thickness S_0 used in this paper promotes the temperature gradient mechanism and thus only makes concave forming possible. But the methodology presented in this paper is applicable to convex or mixed concave/convex forming, where D needs to be a variable as well. The decision variables for the laser-forming problem defined above can, therefore, be represented in terms of a matrix. There are $3\times N$ independent decision variables.

$$E = \begin{bmatrix} P_1 & \cdots & P_N \\ V_1 & \cdots & V_N \\ d_1 & \cdots & d_N \end{bmatrix} \tag{4}$$

The range of the decision variables is chosen as P: [200,900] W and V: [20,90] mm/s. Please note the number of parallel scan lines N is not an independent variable and it is constrained by $\sum_{i=1}^{N} d_i =$ half sheet width. Only half of a sheet is considered assuming symmetry.

Let R_i and θ_i denote the radius of curvature and bending angle as the result of the ith scan, respectively (Fig. 1a). It is also assumed that $d_i \geq R_i\theta_i$, that is, adjacent scan lines do not overlap such that R_i and θ_i are determined solely by the ith scan. The length of the straight portion between arc $R_i\theta_i$ and adjacent arc R_{i+1} θ_{i+1} is denoted as $h_i = d_i - R_i\theta_i$. After the 1st, 2nd and ith scans, coordinates of the partially formed 2D profile can be expressed as:

$$Y_1 = y_1, \quad Z_1 = z_1; \quad Y_2 = Y_1 + y_2\cos\theta_1 - z_2\sin\theta_1,$$
$$Z_2 = Z_1 + y_2\sin\theta_1 - z_2\cos\theta_1 \text{ and}$$
$$Y_i = Y_{i-1} + y_i\cos\left(\sum_{k=1}^{i-1}\theta_k\right) - z_i\sin\left(\sum_{k=1}^{i-1}\theta_k\right),$$
$$Z_i = Z_{i-1} + y_i\sin\left(\sum_{k=1}^{i-1}\theta_k\right) - z_i\cos\left(\sum_{k=1}^{i-1}\theta_k\right) \tag{5}$$

respectively. This equation is derived in the following way. The laser formed 2D profile is assumed to be arcs connected by straight lines tangential to these arcs. Therefore, the coordinates after ith scans are coordinates after $(i-1)$th scans plus the coordinates transformation of ith scans due to the aggregated bending angle, $\sum_{k=1}^{i-1}\theta_k$. The coordinates after ith scans before coordinates transformation are $y_i = R_i\sin(\theta)$, and $z_i = R_i(1-\cos(\theta))$ for the arc section $R_i\theta_i$ and $\theta \in (0,\theta_i)$; $y_i = R_i\sin(\theta_i) + h\cos(\theta_i)$, and $z_i = R_i(1-\cos(\theta_i)) + h\sin(\theta_i)$ for the straight segment h_i and $h \in (0, d_i - R_i\theta_i)$.

The above equations will be used to express the formed shapes in the fitness function, which is part of the GAs to be explained in Section 5.2. Additionally, in the process of applying the GAs, it is necessary to determine θ_i and R_i for candidate design variables P_i and V_i. While this could be achieved via the well-established, full-blown FEM modeling, a more feasible approach is to use empirical relationships based on readily available experimental data since the number of such determination is large as GAs evaluate many candidate values of the design variables. Shown in Figs. 2 and 3 are bending angle θ_i and radius of curvature R_i vs. power and velocity, respectively, based on experimental data of 1010 steel coupons of 80 by 80 by 0.89 mm with beam size of 4 mm, the same condition to be

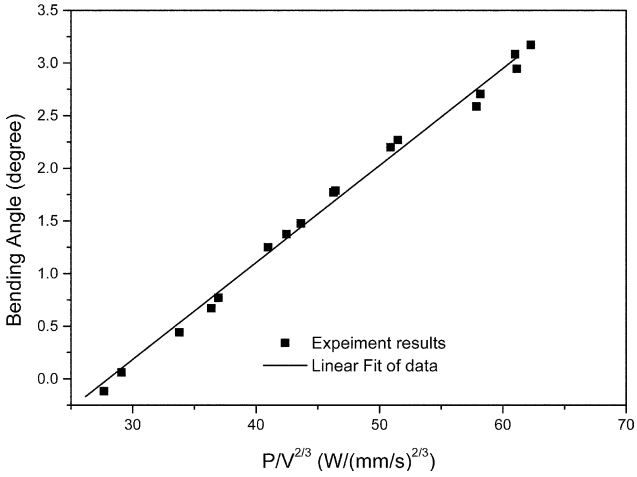

Fig. 2. Linear fit of bending angle and $P/V^{2/3}$ from experimental results.

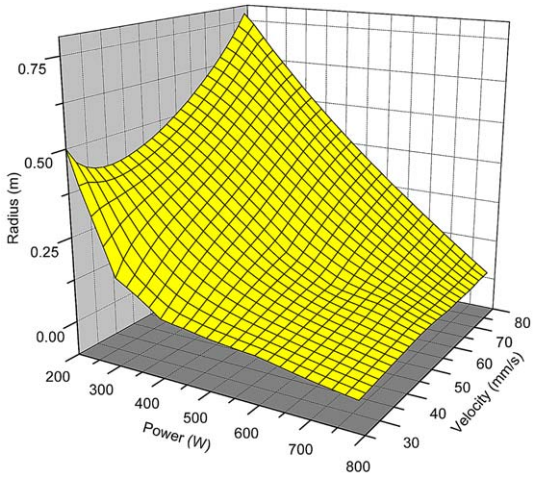

Fig. 3. Relationship of heat conditions and radius of curvature from experimental/numerical study.

used in the paper. As seen from Fig. 2, bending angle correlates linearly with $P/V^{2/3}$. This result may somewhat differ from others [1,15], but it conveniently serves the purpose of this paper since the conditions under which the two figures are constructed are the same as the ones being considered in this paper.

4. Genetic algorithms

GAs are a class of stochastic search methods that mimic the metaphor of natural biological evolution. GAs operate on a population of potential solutions applying the principle of survival of the fittest to produce better and better approximations to a solution, just as in natural adaptation. The basis steps of implementing GAs are summarized in Fig. 4 with more discussions in Section 5. First, generate a random population of N_p; second, evaluate the fitness of each chromosome in the population and create a new population by repeating the following steps until the new population is complete: (a) select parent chromosomes from a population according to their fitness (the better fitness, the higher chance to be selected; (b) with a crossover probability, cross over the parents to form a new offspring; (c) with a mutation probability mutate the new offspring at each locus (position in chromosome); (d) place new offspring in a new population; (e) use newly generated population for a further run of algorithm; (f) if the end condition is satisfied, stop, and return the best solution in current population.

How to choose the control parameters (such as population size, crossover rate, mutation rate, representation of decision parameters and others) is important to the performance of GAs. There have been studies investigating the interactions among different GA parameters for successful application of GAs [16] and control maps for operator probabilities [17,18]. But their interactions are largely dependent on the function being optimized and therefore only general guidelines are appropriate, which are briefly summarized below for the self containment of the paper.

Population size is the first parameter to choose. Generally, a highly undulating cost surface should have a larger population than a smooth cost surface. There is always a trade-off between the number of generations the algorithm needs to converge vs. the size of the population. A small population size causes the GA to quickly converge to a local optimum, while a large population size takes too long to find and assemble the building blocks to the optimum solution. The number of evaluations, that is, the produce of population size and the number of generations required to converge, is a good measure of the algorithm efficiency. Grefenstette [19] used genetic algorithm to optimize genetic

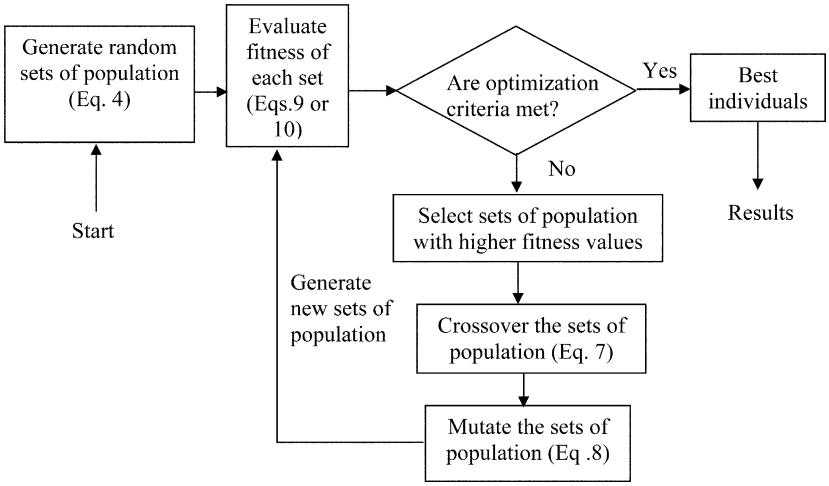

Fig. 4. The basis steps of implementing GAs.

algorithm parameters. Unfortunately, the optimum parameters for one problem are not the optimum parameters for another. He also found that relatively large populations are good for parallel implementations of the GA, while relatively small populations are good for serial implementations. The most effective population size is dependent on the problem being solved, the representation used, and the operator manipulating the parameters [20]. Mühlenbein [21] modeled the GAs based on Markov chain analysis. He calculated the transition probability of moving to the optimal string from any string and then estimated the expected transition time. He showed that this transition probability reduces with population size, giving rise to the concept of a minimum population size below which GAs are not expected to work. Goldberg et al. [16] showed that a population size N_p is necessary to trigger correct building block processing based on correct schema processing:

$$N_p = 2ck\sigma_0^2/f_0^2 \tag{6}$$

where f_0 and σ_0 are the mean and variance of the fitness values, respectively; k is the number of competing schemas; and the factor c varies with error rate $\alpha = \exp(-c/2)/\sqrt{2\pi c}$.

Crossover operator is a constructive process, which can combine good partial solutions together to form the optimal solution. The goal of the crossover operator is to pass on desirable traits to the next generation. Crossover rate C determines the number of chromosomes that enter the mating pool. If crossover rate is too high, good building blocks do not have the opportunity to accumulate within a single chromosome. A low crossover rate, on the other hand, does not do much exploring of the cost surface. By mutation operator, offspring variables are mutated by small random values. Bäck [22] reported that for unimodal functions a mutation rate of $1/N_p$ was the best choice. This value may be still valid when fitness function is multimodal. Generally, with a small mutation rate, the algorithm is easy to converge to local optima, while a large mutation rate destroys the already-found building blocks. In practice, these control parameters are often determined semi-empirically on a case-by-case basis in order to minimize the number of evaluations required, which is the product of population size and the generations that take to converge. How these control parameters are chosen will be illustrated in the next section.

5. Results and discussions

As explained in Section 3, the sheet dimension is $80 \times 80 \times 0.89$ mm, and the laser beam diameter is 4 mm. Only half of the sheet is scanned (Fig. 1(b)). The class of target shapes is characterized by a profile on the Y–Z plane and the profile remains unchanged in the X direction (Fig. 1). The 2D target profiles investigated in the paper include a circular profile of constant radius of 0.1 m and a parabolic profile $z = 8y^2$. The former has a constant curvature while the latter a varying curvature. The scanning pattern is straight-lines and parallel to each other and parallel to the X-axis.

5.1. Optimal GA parameters for the problem

To choose the best GA parameters for process design of laser forming process, the following case is considered. The target shape is the circular profile mentioned above. Due to its constant radius of curvature, $P_i = P$ and $d_i = d =$ half of the sheet width$/N$ are assumed. The scanning velocity is set as a constant, $V_i = V = 50$ mm/s, and therefore P and N are the two design variables to be determined.

To choose the optimal population size, the crossover rate, C, and mutation rate, M, are chosen as 0.8 and 0.05, respectively, while the population size varies from 5 to 500. Fig. 5(a) shows the development of the fitness function value (Eq. (7)) with generation for several population sizes. The fitness is evaluated using the following fitness function

$$f_1 = \left(1 \Big/ \left(1 + \int_0^l \frac{|f(y) - f_0(y)|\mathrm{d}y}{lS_0}\right)\right)^N \tag{7}$$

where $f(y)$ represents the formed shape function, $f_0(y)$ is the target shape function, S_0 is the sheet thickness, l is the sheet length, and N is the number of scan lines. $|f(y)-f_0(y)|$ specifies the vertical difference between the formed and target surfaces for the same y coordinate. The result shows that the number of generations to achieve convergence decreases with increasing population size, which is consistent with many previous studies using GAs [11,16]. The minimum population size below which GAs are not expected to work (Eq. (6)) is determined as 17. The mean and variance of the fitness values $\bar{f}_0 = 0.26$, and $\bar{\sigma}_0 = 0.59$ were obtained by sampling 1000 chromosomes randomly generated. $k = 1$, and $c = 1.67$ (with 90% confidence) were used (Eq. (6)). Figs. 5(b) and (c) show that GAs with about $N_p = 20$ work the best for the chosen crossover and mutation rates because they give the lowest number of evaluations.

Fig. 5(b) also shows the effect of crossover rate on the convergence speed at different population sizes. Mutation rate is set as 0.05 and crossover rate varies from 0 to 1. The number of evaluation when crossover rate is 0.5 is much larger than that when crossover rate is large ($C = 0.8$ or 1). The GAs do not converge when crossover rate is 0 or 0.1. This is because crossover operator is a constructive process, which can combine good partial solutions together to form the optimal

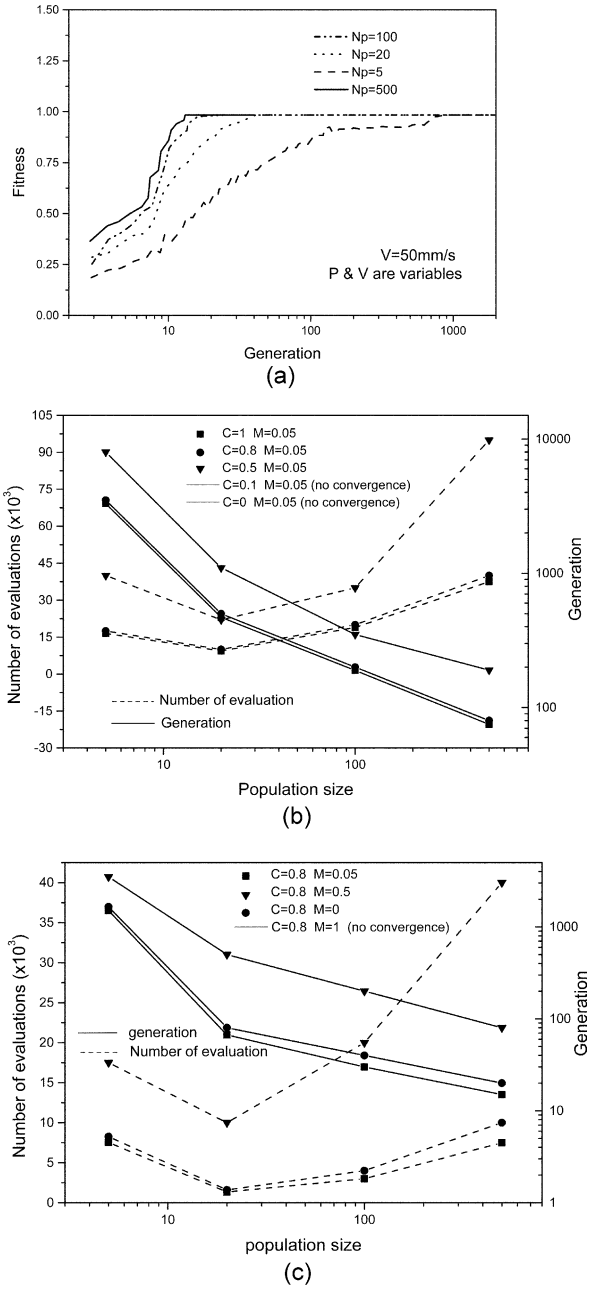

Fig. 5. (a) Effect of population size N_p on fitness convergence; (b) effect of crossover rate on the number of generations and number of evaluations ($= N_p \times$ generations); (c) effect of mutation rate on the number of generations and number of evaluations.

solution. There is slight difference in convergence speed between crossover rate of 0.8 and 1.

A similar approach was applied to investigate the effect of mutation rate on the convergence. Crossover rate is set as 0.8 here (Fig. 5(c)) while mutation rate varies from 0 to 1. As seen, $M = 0.05$ gives the lowest number of evaluations at population size about 20. The GAs do not converge when mutation rate is 1. This is because a large mutation destroys the already-found building blocks in a population. The results from Bäck [22] help confirm the observation. He concluded that if cost function is a uni-modal pseudoboolean function, mutation rate $M = 1/N_p$ is the best choice. When the fitness function becomes multi-modal, mutations rate $M = 1/N_p$ is still valid to overcome local optima, when crossover is introduced. In this case, when population size is about 20, the best mutation rate is about $1/20 = 0.05$.

These results show that if the population size is adequate, a combination of large crossover with a small mutation provides efficient evolution (convergence). Specifically, for this case, the best set of control parameters is population size about 20, high crossover rate (larger than 0.8), and low mutation rate (smaller than 0.05).

5.2. Fitness function

The selection of fitness function has to be consistent with the nature of the problem at hand and the objective of the optimization. In this study, the issues concerned the most are geometry accuracy, total forming time, and energy consumption. Based on these considerations, two fitness functions are formulated.

The first fitness function was shown in Eq. (7) in Section 5.1. The geometry and number of scans are considered. As seen, the optimal fitness value is 1 when $f(y)$ equals $f_0(y)$. The fitness value decreases as the number of scans increases and the shape difference increases. A large number of N favors geometry accuracy but generally consumes more time.

The second fitness function is

$$f_2 = \alpha \Big/ \left(1 + \int_0^l \frac{|f(y) - f_0(y)|\mathrm{d}y}{lS_0}\right) + \beta \left[\sum_{i=1}^{N} \frac{P_i l_i}{V_i}\right]_{\min} \Big/ \sum_{i=1}^{N} \frac{P_i l_i}{V_i} \tag{8}$$

P_i, V_i, and l_i are power, scanning velocity and length of the ith scanning path, respectively. $P_i l_i / V_i$ is the energy consumption at the ith scan. $[\sum_{i=1}^{N} P_i l_i / V_i]_{\min}$ is the minimal total energy consumption among all the strings in a generation. The first item of this fitness function measures the fitness associated with geometry accuracy weighted by α; and the second item energy consumption weighted by β, and $\alpha = 1 - \beta$.

To compare the effect of optimization results using these two fitness functions, f_2 was applied to the case of $V = 50$ mm/s as dealt with in Section 5.1. In Section 5.1, the results shown in Figs. 5 and 6 were obtained using the fitness function f_1. Fig. 7 compares the development of the number of scans and power with generations using the two fitness functions. In fitness function, f_2, α and β are both set as 0.5. The results show that N converged to 14 using f_1 (the same as in

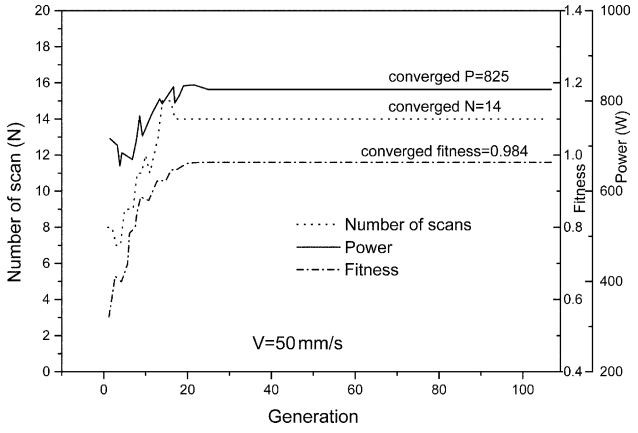

Fig. 6. The development of fitness and decision variables (number of scan lines and power) during GAs optimization with V set as 50 mm/s.

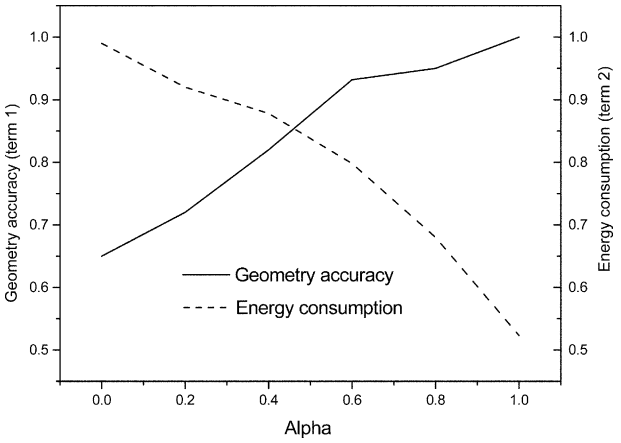

Fig. 8. Effects of weighting coefficients in the second fitness function (Eq. (10)) on the fitness of geometry accuracy (the first term in Eq. (10)) and energy consumption (the second term in Eq. (10)).

Fig. 6(a)), and converged to 10 using f_2. The corresponding P converged to 825 W (the same as in Fig. 6(a)) and 846 W, respectively. The converged fitness f_1 and f_2 are 0.994 (Fig. 6(a)) and 0.84 (not shown), respectively. It is seen that with f_1, the GA results have better geometric accuracy while the energy consumption is higher. If the formulation of the second term in Eq. (10) is used, the fitness of energy consumption is about 0.64. With f_2, however, the GA results have better energy consumption while compromising the geometry accuracy somewhat. If Eq. (9) is used, the fitness of geometric accuracy is about 0.865. The result under f_2 naturally varies with the choice of α and β $(= 1 - \alpha)$ value. Fig. 8 shows the effect of α on the balance between the fitness associated with geometry accuracy (the first term in Eq. (10)) and energy consumption (the second term in Eq. (10)). It is seen that the converged geometry accuracy increases and energy consumption fitness decreases with increasing α. The fitness function, therefore, should be carefully chosen to have results that best reflect the process designer's priorities.

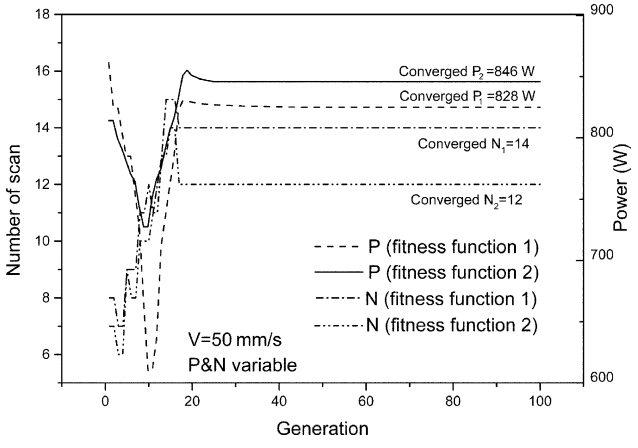

Fig. 7. Comparison of fitness function effects on GAs optimization results (fitness functions 1 and 2 are specified by Eqs. (9) and (10)).

5.3. Overall strategy of process synthesis of laser forming

With optimized control parameters and carefully chosen fitness function, the GA optimization of laser forming process is implemented in four steps. (1) An initial set of 20 chromosomes is randomly generated within a range. Each chromosome represents a scanning pattern and heat condition in terms of $3\times N$ decision variables as described in Section 3. The range for P is chosen as 200 to 900 W based on the prior knowledge of the deformation/power relationship and the desired shape. The range for N is chosen as 5–15 based on the fact that no significant overlapping of scan lines is desired, and the sheet metal half width and laser beam size D are 40 and 4 mm, respectively. (2) The fitness of the 20 chromosomes is evaluated using the fitness function shown in Eq. (7) because geometry accuracy is the first priority in this study. Ten chromosomes having the highest fitness values are chosen. Eight of these 10 chromosomes $(C = 0.8)$ crossover with other 8 out of 10 randomly generated chromosomes to generate new chromosomes according to

$$E_{ij}^{\text{new}} = r_c E_{ij}^1 + (1 - r_c) E_{ij}^2 \tag{9}$$

where E_{ij}^1 and E_{ij}^2 are one of the 8 best chromosomes and one of the 8 randomly generated chromosomes, respectively (also see Eq. (4)); and r_c is a random number from a (0,1) uniform distribution. (3) The new set of 20 chromosomes (16 crossovered ones and four uncrossovered ones) are then mutated according to

$$E_{ij}^{\text{mutate}} = U(a_i, b_i) \tag{10}$$

where a_i and b_i are the range of the ith decision variable. $U(a_i,b_i)$ is a randomly generated value from (a_i,b_i) uniform distribution. (4) The new set of offsprings after selection, crossover and mutation operators, are chosen for the next generation. Steps 2 and 3 are repeated until a global convergence measure is achieved. The global convergence is assumed if no improvement in the fitness value takes place after a fixed number of trials, which is set as 20 in this study. With these steps, convergence to $P = 825$ W and $N = 14$ was achieved in about 20 generations with a fitness value of 0.984 (Fig. 6) in the above case with circular profile as target shape (radius = 0.1 m) and V is set as 50 mm/s. The overlapping of adjacent scans is avoided since interval between scans $d_i \geq R_i\theta_i$. $R_i\theta_i$ is around 0.4 mm under conditions of $P = 825$ W, $V = 50$ mm/s, while $d_i = d = 40(\text{half plate width})/14(\text{or } 18)$ is larger than 2 mm. The constraint of the decision variable is $25 \leq P/V^{2/3} \leq 65$ because it is shown in Fig. 2 that the linear relationship between bending angle and $P/V^{2/3}$ is with a range. As we discussed in Section 3, the final shape is decided by the aggregated bending angle and curvature, which are both functions of power and velocity. Therefore, if the number of scans is variable, there could be different combination of power and velocity for a target shape.

5.4. Two case studies with experimental validation

5.4.1. Case 1: circular profile in Y–Z plane (P and V variables, N and d constants)

To test the algorithm's applicability under other conditions, two case studies were conducted. In the first case, laser heating power is a constant variable, $P_i = P$, velocity is a constant variable, $V_i = V$, and the number of scans N is set constant equal to 10. Therefore, there are two decision variables P and V. d_i = half sheet width$/N = 40/10 = 4$ mm. The target shape remains as a circular profile with diameter of 0.1 m in the Y–Z plane (Fig. 9). Fig. 10(a) shows the development of the decision variables, P and V, as well as the fitness value during the GA optimization. Fig. 9 shows the shape

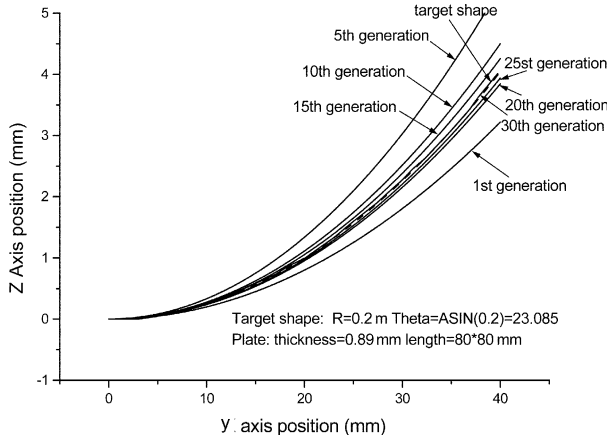

Fig. 9. The development of shape during optimization process of GAs (Case 1).

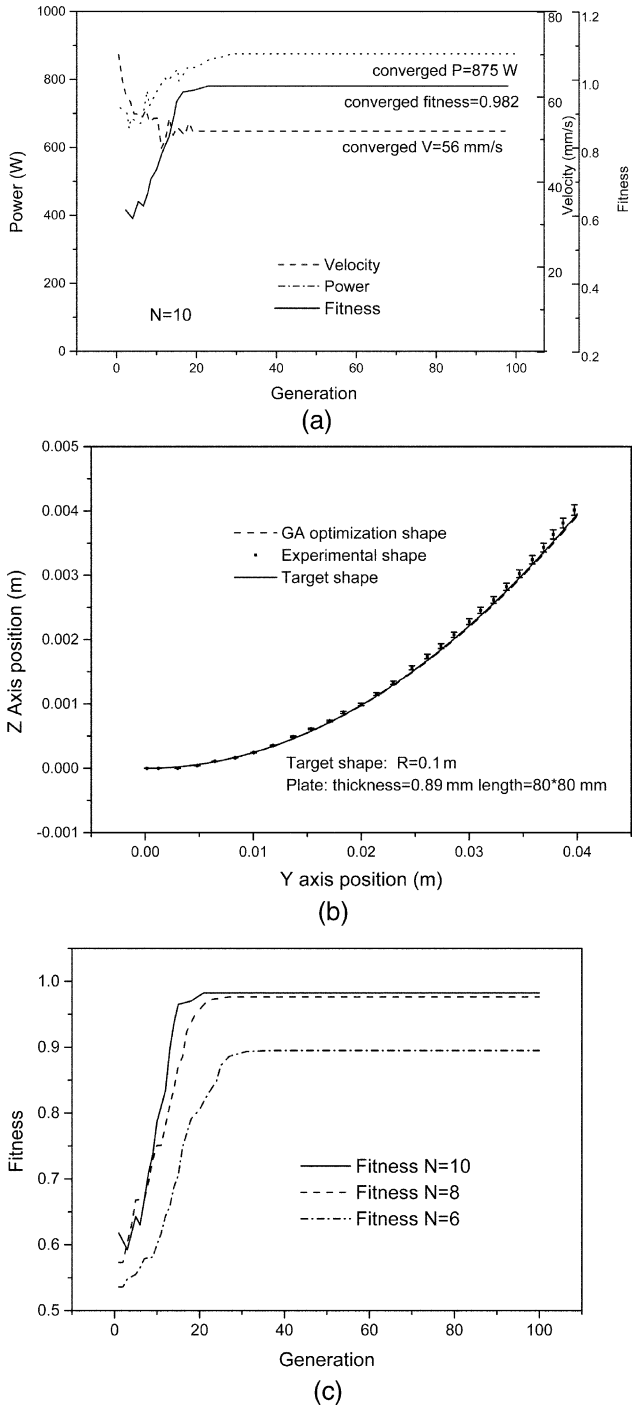

Fig. 10. (a) Convergence history of decision variables P and V, and fitness with $N = 10$; (b) comparison of shapes from GA optimization, experimental and target; and (c) convergence history of fitness when $N = 6$, 8, and 10, respectively.

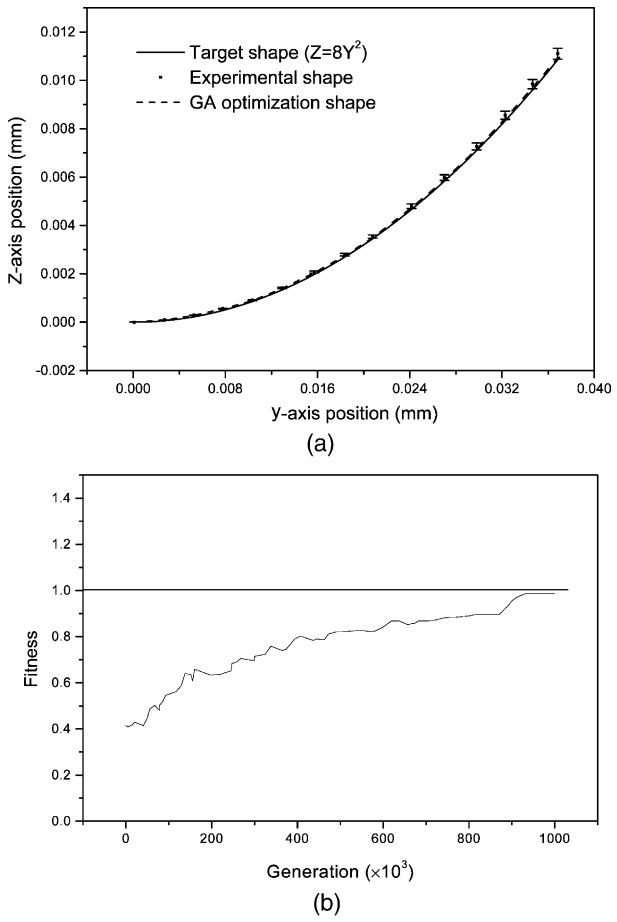

Fig. 11. (a) The comparison of shapes from GAs optimization, target and experiment; and (b) the development of fitness during GAs optimization, the converged result is close to optimal (Case 2).

evolution during the optimization process of GA. The results in Figs. 9 and 10a show that when the number of generations reaches about 30, the shape from GAs optimization is very close to the target shape, and P and V converge to optimal values of 875 W and 56 mm/s, respectively. Fig. 10(a) also shows that the fitness of the converged results is close to optimal, 0.982.

To validate the solutions from the GA optimization, an laser forming experiment was conducted under the same conditions. The shape after laser forming is compared with the target shape as shown in Fig. 10(b). The formed shape is then measured by a coordinate measuring machine (CMM). Three samples were formed and error bars were added in Fig. 10(c). It shows that the shape after laser forming is close to the target shape. Therefore, the GA optimization is proven to be a valid method to solve the process design problem for the target shape. To test the validity under different predetermined number of scans, GA optimization was conducted with the number of scans of 6 and 8 and the convergence history of fitness is shown in Fig. 10(c). As seen, when the number of scans is 10 and 8, the fitness approaches the optimal value of 1 and for $N = 6$ to a value less than 1. It is obvious that for a smaller number of scans, the closeness between the target and actual shapes is limited.

5.4.2. Case 2: parabola profile in Y–Z plane (d_i and P_i variables, V and N constants)

This case assumes a parabolic target shape of $z = 8y^2$, whose radius of curvature increases with Y (Fig. 11(a)). As a result, the intervals between scans, d_i, and powers of each scan, P_i, are chosen to be variables from scan to scan. The number of scans, N, is set to 15, and the scanning velocity of each scan is set as $V_i = V = 50$ mm/s. As a result, the total number of decision variables is 29, that is P_i and d_i ($i = 1$–15) but

Table 1
GA optimization results (Case 2)

$N = 15$			$N = 12$			$N = 8$		
No.	d_i (mm)	P_i (W)	No.	d_i (mm)	P_i (W)	No.	d_i (mm)	P_i (W)
1	2.504	682.8	1	3.197	754.4	1	4.848	859.3
2	2.512	679.2	2	3.208	748.3	2	4.867	852.1
3	2.518	675.8	3	3.215	743.5	3	4.921	846.5
4	2.527	672.6	4	3.227	738.2	4	4.957	841
5	2.555	670.6	5	3.263	733.6	5	4.993	837.3
6	2.574	668.8	6	3.287	729.5	6	5.066	835
7	2.593	666.9	7	3.311	725.8	7	5.138	832.6
8	2.63	665.2	8	3.359	722.5	8	5.21	830.2
9	2.668	663.8	9	3.407	719.4			
10	2.705	662.5	10	3.455	716.3			
11	2.743	661.4	11	3.503	713.2			
12	2.79	660.3	12	3.563	710.6			
13	2.837	659						
14	2.893	657.8						
15	2.95	656.1						
	Converged fitness 0.978			Converged fitness 0.972			Converged fitness 0.885	

summation of all d_is equals the half sheet width of 40 mm. The left side of Table 1 lists the design results from the GA optimization. As seen, d_i increases and P_i decreases with the scan number (towards larger Y values) in order to match the increasing radius of curvature of the target shape. Fig. 11(a) shows a good agreement between the shape from GA optimization and the target shape. Fig. 11(b) shows that the fitness of the converged results is close to optimal, 0.978, but only after a much larger number of generations than in the other two cases, simply because of the larger number of decision variables in this case. This case shows that when the profile of the target shape is more complex and the number of decision variables is large, the algorithm converges but with a large time premium. Similarly, experiments were conducted under the conditions from the GA optimization, and results were superimposed in Fig. 11(a). The experimental shape agrees reasonably well with the target shape. To test the validity under different predetermined number of scans, GA experiments were conducted with the number of scans of 8 and 12. The results are shown in the mid and right side of Table 1. When the number of scans is 12 or 8, the fitness also converges but to slightly smaller values as expected.

6. Conclusions

In this paper, a synthesis process for laser forming of sheet metal based on GAs is presented. It was demonstrated through this investigation that given a desired shape for the class of shapes concerned, the present approach is effective in determining the optimal values of diverse process parameters for laser forming process. It was also shown that it is able to handle a large number of decision variables. When the number of decision variables was close to 30, however, it took a large number of generations to achieve convergence. Investigations showed that the algorithm control parameters and the fitness function type have significant effects on the GA synthesis results. It is shown that a proper form of fitness function is important to balance among competing objectives, such as geometric accuracy, forming time, and energy consumption.

Acknowledgements

Support for this project under an NSF grant (DMI-0000081) is gratefully acknowledged. Insights of GA implementations provided by Prof. D.E. Goldberg of University of Illinois at Urbana-Champaign are also greatly appreciated.

References

[1] F. Vollertsen, Mechanism and models for laser forming, Proceedings of the Laser Assisted Net Shape Engineering (LANE '94), vol. 1, 1994, pp. 345–360.
[2] Y. Hsiao, et al., Finite element modeling of laser forming, Proceedings of the ICALEO '97, Section A, 1997, pp. 31–40.
[3] J. Magee, K.G. Watkins, W.M. Steen, Advances in laser forming, Journal of Laser Application 10 (1998) 235–246.
[4] J. Bao, Y.L. Yao, Analysis and predication of edge effects in laser bending, Proceedings of the 18th International Congress on Applications of Lasers and Electro-Optics (ICALEO '99): Conference on Laser Materials Processing, San Diego, CA, Section C, 1999, pp. 186–195.
[5] W. Li, Y.L. Yao, Numerical and experimental study of strain rate effects in laser forming, ASME Transactions, Journal of Manufacturing Science and Engineering 122 (3) (2000) 445–451.
[6] W. Li, Y.L. Yao, Numerical and experimental investigation of convex laser forming process, ASME Journal of Manufacturing Processes 3 (2) (2001) 73–81.
[7] J. Cheng, Y.L. Yao, Microstructure integrated modeling of multiscan laser forming, ASME Transactions, Journal of Manufacturing Science and Engineering 124 (2) (2002) 379–388.
[8] H. Shimizu, A heating process algorithm for metal forming by a moving heat source, M.S. Thesis, MIT, 1997.
[9] T. Hennige, Development of irradiation strategies for 3D laser forming, Journal of Materials Processing Technology 103 (1) (2000) 102–108.
[10] J. Magee, K.G. Watkins, T. Hennige, Symmetrical laser forming, Proceedings of the ICALEO, Section F, 1999, pp. 77–86.
[11] D.E. Goldberg, Genetic Algorithms in Search, Optimization and Machine Learning, Addison-Wesley Publishing Company, Inc, 1989.
[12] L. Davis, Handbook of Genetic Algorithms, Van Nostrand Reinhold, New York, 1991.
[13] J.S. Chung, S.M. Hwang, Application of a genetic algorithm to process optimal design in non-isothermal metal forming, Journal of Material Processing Technology 80–81 (1998) 136–143.
[14] S. Roy, et al., Optimal design of process variables in multi-pass wire drawing by genetic algorithms, Journal of Manufacturing Science and Engineering 118 (1996) 244–251.
[15] K. Masubuchi, Studies at M.I.T. related to applications of laser technologies to metal fabrication, Proceedings of the LAMP '92, 1992, pp. 939–946.
[16] D.E. Goldberg, et al., Genetic algorithm, noise, and the sizing of populations, Complex System 6 (1992) 333–362.
[17] D.E. Goldberg, et al., Massive multimodality, deception, and genetic algorithm, Parallel Problem Solution in Nature 2 (1992) 37–46.
[18] D. Thienrens, D.E. Goldberg, Mixing in genetic algorithm, Proceedings of the Fourth International Conference on Genetic Algorithms, 1993, pp. 38–45.
[19] J.J. Grefenstette, Optimization of control parameters for genetic algorithms, IEEE Transactions on Systems, Man and Cybernetics, vol. SMC-16, No. 1, 1986, pp. 122–128.
[20] G. Syswerda, A study of reproduction in generational and steady-state genetic algorithms, in: G.J.E. Rawlins (Ed.), Foundations of Genetic Algorithms, Morgan Kaufmann Publishers, San Mateo, CA, 1991, pp. 94–101.
[21] H. Mühlenbein, How genetic algorithm really work: I. Mutation and hillclimbing, in: G.J.E. Rawlins (Ed.), Foundations of Genetic Algorithms, Morgan Kaufmann Publishers, San Mateo, CA, 1992, pp. 15–25.
[22] T. Bäck, Optimal mutation rates in genetic search, in: S. Forrest (Ed.), Proceedings of the Fifth International Conference on Genetic Algorithms, Morgan Kaufmann Publishers, San Mateo, CA, 1993, pp. 2–8.